Engineering Immune-Evasive Artificial Blood Using Q31P-Modified CD47 Protein Coating to Extend Circulation Lifespan

Aryan Katakam[1], **Ashvath Katakam**[1]

Received July 14, 2026
Accepted October 18, 2026
Electronic access November 30, 2026

Background/Objective: Artificial Red Blood Cells containing yeast-produced hemoglobin are a scalable alternative for donor blood; however, they can be cleared by the immune system via macrophages. CD47 is a membrane protein which, when it interacts with the SIRPα receptor, inhibits the phagocytic activity of macrophages. Q31P is a variant of CD47 that retains SIRPα binding but also shows reduced binding to specific therapeutic antibodies against CD47. However, there has been no assessment of whether this protein can be used as a coating on Artificial Red Blood Cells. In this work, we have developed a theoretical model to simulate the lifetime in circulation of ARBCs coated with Q31P-CD47 and to estimate the conditional surface-density requirements of Q31P-CD47.
Methods: A first-order exponential pharmacokinetic model was parameterized using two verified in vivo circulation half-lives. The Selective Immune Camouflage Index (SICI) was calculated for three different CD47 variants using previously reported values. An illustrative surface-density design model based on the Hill equation was used to estimate conditional ARBC surface-coating requirements.
Results: A30P scores higher than Q31P (1.461 vs. 1.258), reflecting greater SIRPα binding in the SICI calculation. In addition, under an antibody-challenge scenario involving the anti-CD47 monoclonal antibody B6H12, Q31P had a binding-selectivity advantage because it exhibited near-zero reactivity with B6H12. The conditional design target for Q31P molecules per ARBC was approximately 2,700–4,800.
Conclusions: This framework is based on published data to provide quantifiable ARBC coating requirements and represents a computational approach that, to our knowledge, has not previously been reported in this form, including which CD47 variant to use, the minimum coating density required, and the clinical context in which each variant is preferred. All predictions are directly experimentally testable.

Keywords: artificial red blood cells, CD47, SIRPα, Q31P, immune evasion, SICI, pharmacokinetics, Hill equation, surface density, macrophage phagocytosis

Introduction

Background and Context

The global blood supply has been under pressure from the need for blood type matching, storage limitations due to limited shelf life, and reliance on volunteer blood donors. These are all factors that negatively impact emergency situations and resource-constrained environments. To alleviate some or all of these pressures, researchers have developed artificial blood products (blood substitutes)[1–3]. These products are meant to mimic the ability of natural red blood cells (RBCs) in carrying oxygen. Recent examples of this emerging field are created using yeast and can be manufactured in large quantities without depending on individual donations[4]. Further, their surfaces may be engineered with custom molecular coats[5].

One major obstacle to the clinical translation of artificial red blood cell (ARBC) carriers is their limited circulation lifespan. Foreign particles are removed by macrophages of the mononuclear phagocyte system (MPS), often in just a matter of hours[6]. Healthy human erythrocytes have an average lifetime of around 115-120 days; most synthetic particles do not approach such longevity. CD47, a transmembrane protein with a glycosylated extracellular domain expressed on all normal host cells, is the main "do not eat" signal responsible for suppressing macrophage-mediated phagocytic clearance by engaging inhibitory receptor SIRPα[7–11]. Researchers have demonstrated that coating PLGA nanoparticles with native erythrocyte membranes (which contain surface-expressed CD47) results in a 2.5 fold increase in circulation half life as compared to PEGylation (39.6 h versus 15.8 h in mice)[12,13]. This study established that using CD47 to create membrane camouflage provides superior protection against phagocytic

[1] *American High School, USA*

© The National High School Journal of Science 2026

recognition than does current stealthy synthetic approaches to reducing particle recognition [14 15–17].

The synthetic microparticle modeled in this study is a hypothetical synthetic microsphere with a lipid-based shell. The modeled particle diameter ranged from 2-10 μm. Each particle was assumed to encapsulate recombinant hemoglobin produced using a yeast-based expression system. However, yeast is not part of the final ARBC carrier; it serves solely as the production platform for recombinant hemoglobin. On the outer surface of the lipid membrane, an engineered CD47 protein variant called Q31P-CD47 is modeled as attached either through random chemical conjugation or through coating with membranes derived from CRISPR-engineered cells expressing CD47 as a transmembrane protein. This exact ARBC design has not yet been experimentally produced and should therefore be understood as a hypothetical carrier whose feasibility is evaluated computationally in this study.

Problem Statement and Rationale

While native CD47 provides effective immune camouflage, it is also the target of clinically used anti-CD47 antibodies (B6H12, TJC4, Hu5F9), which block the CD47-SIRPα axis to re-sensitize cancer cells to phagocytosis [18–22]. Consequently, any synthetic therapeutic particle bearing native CD47 will be stripped of its protective signal by anti-CD47 antibodies present during treatment with these drugs. Therefore, Yamada-Hunter et al. [23] proposed an approach to avoid this problem when modifying CAR-T cells with a Q31P substitution in CD47 that preserves binding to SIRPα but eliminates recognition by anti-CD47 antibodies like B6H12. However, no studies have evaluated the performance of this variant on artificial red blood cells or generated quantitative models for how well this variant would protect ARBCs.

Significance and Purpose

The framework for determining how well a particular Q31P-CD47 will perform with ARBCs would allow engineers to make more informed decisions before conducting expensive in vivo experiments: which variant to use; how many molecules to coat per cell; and what patient populations will be best served. In this paper we develop a framework that integrates the two previously disconnected datasets: verified in vivo circulation half-lives and multi-variant CD47 binding selectivity data into a unified quantitative model.

Objectives

The focus of this study is based on three key areas for investigation. The first area includes the estimation of the circulation half-life for Q31P-CD47-coated ARBCs as well as the impact that alterations in assumed coating efficacy have on predictions regarding half-lives. The second area compares the A30P, Q31P and knockout forms of CD47 by using a novel dual-receptor selectivity metric to identify the most effective form of immune camouflage. The third area establishes an estimate of the minimum surface density of Q31P-CD47 required to inhibit macrophage activity against yeast derived ARBCs and assesses variables (e.g., ARBC diameter, orientation) impacting these requirements.

Scope and Limitations

This study is fully computational and predictive. No in vitro or in vivo experimentation was done for this project. All of the parameters used to make model predictions have been taken from other studies. Therefore, any predictions made by our models depend upon the validity of the assumptions outlined in the Methods section. The discussion section outlines these assumptions, which are explicitly acknowledged and quantified.

Theoretical Framework

Two established modeling frameworks were used: (1) First order exponential pharmacokinetic decay was used for modeling ARBCs clearance; and (2) Hill equation based on receptor occupancy theory to model the relationship between surface CD47 density and macrophage SIRPα engagement [24].

Methodology Overview

Circulation half-life data from Hu et al. [12] and the CD47 binding and phagocytosis data from Yamada-Hunter et al. [23] were entered into a MATLAB computational model. A novel selectivity metric (Selective Immune Camouflage Index; SICI) was computed for three variants of CD47. A Hill equation model was fitted to the phagocytosis rates and CD47 molecule counts to find the least amount of ARBC coating requirements.

Methods

Research Design

The study used two previously published experimental datasets to perform a predictive model. Therefore, this was a secondary data analysis study using previously published experimental data to build computational models. There were no animals or humans in the study and no new experimental data were collected.

Data Collection

Dataset 1 — Circulation half-lives. Hu et al. [12] found that following intravenous injection in mice, the mean in-vivo half-

© The National High School Journal of Science 2026

lives were $t_{1/2}$ = 15.8 h for those particles which were PEG-coated, and $t_{1/2}$ = 39.6 h for those which had been coated with native erythrocyte membranes. The first is used as the effectiveness anchor at 0%, while the second is used as the effectiveness anchor at 100%.

It is also important to recognize that Hu et al. coated their particles with complete native erythrocyte membranes instead of using purified CD47 alone. Therefore, the improvement in circulation observed in their study reflects the combined contributions of all membrane-associated proteins and cannot be attributed exclusively to CD47. Another distinction was the size of the particles: Hu et al. studied nanoparticles that were less than 100 nm in diameter; however, this study models ARBCs ranging in size from 2–10 μm. Since there are numerous variables associated with how quickly ARBCs will be removed from the bloodstream, including particle size, particle shape, membrane composition, and rigidity among others, the half-lives determined by Hu et al. cannot be directly transferred to the modeled ARBC system. As such, these values will serve as boundary reference points for the application of the scenario analysis described above, but they do not represent measured ARBC-specific pharmacokinetic parameters. In addition, Hu et al. evaluated their original experimental results utilizing a two-compartment pharmacokinetic model while this study utilizes a first-order exponential decay model. This has implications for interpreting Fig. 1 as it represents an illustrative calculation and does not represent a reconstruction of the experimental circulation profile obtained during Hu's original study.

Dataset 2 — CD47 variant binding and phagocytosis data. Yamada-Hunter et al.[23] provided, in Source Data accompanying Extended Data Figs. 7b and 4a–4c: (i) triplicate flow-cytometry binding measurements to hSIRPα (100 nM) and B6H12 antibody (500 nM) for CD47 variants A30P, Q31P, and KO, normalized to wild-type CD47; (ii) macrophage phagocytosis rates for untreated and B6H12-blocked conditions across three donors in triplicate; and (iii) CD47 molecule counts per cell for Q31P-expressing CAR-T cells at Day 4 post-activation in triplicate.

A third candidate data point — a ∼30 h circulation half-life for uncoated yeast ARBCs — was excluded after the cited source (PMC2738310) could not be verified to contain this figure.

Variables and Measurements

Primary variables: circulation half-life ($t_{1/2}$, hours); clearance constant (k, h^{-1}); SIRPα-binding retention (S); antibody-binding retention (A); SICI composite score; effective CD47 surface density (ρ_{eff}, molecules/μm^2); 2D binding constant (ρ_{half}, molecules/μm^2); phagocytosis rate (P,%); receptor occupancy (θ). Correction factors: protein orientation (f_{orient}), steric occlusion (f_{steric}), membrane curvature (f_{curv}). All binding values are dimensionless ratios normalized to wild-type CD47 (WT = 1.0).

Procedure

Step 1: Pharmacokinetic model. Clearance constants were derived as $k = \dfrac{\ln(2)}{t_{1/2}}$ for both reference conditions. An effectiveness-scaling interpolation defined predicted half-life for Q31P-coated ARBCs as:

$$t_{1/2}(\text{eff}) = t_{1/2,\text{PEG}} + \left(t_{1/2,\text{RBC}} - t_{1/2,\text{PEG}}\right) \times \left(\frac{\text{eff}}{100}\right) \quad (1)$$

Four effectiveness scenarios were evaluated: 50%, 70%, 100%, and 125%. These values represent assumptions for the fraction of the circulation benefit due to the RBC membrane that might be achievable by utilizing a CD47 based-coating as opposed to measured data. The 125% value is an extension beyond the available reference data; this value should therefore be viewed with caution.

Step 2: SICI definition and calculation. The Selective Immune Camouflage Index was defined as:

$$\text{SICI} = S \times (1 - A) \times \left(\frac{\text{HQ31P}}{H_{\text{ref}}}\right) \quad (2)$$

where S is SIRPα-binding retention, A is antibody-binding retention, and H/H_{ref} is the predicted circulation half-life ratio normalized to the native-CD47 reference (39.6 h). The formulation is multiplicative so that failure on either binding axis, loss of S or gain of A, collapses SICI to zero. SICI was computed for A30P, Q31P, and KO using $H/H_{\text{ref}} = 1.0$ (100% effectiveness projection). SICI scores are being utilized here as an approximate index for binding specificity as opposed to providing actual predictions of in-vivo circulation or determining clinical preference. H/Ref was added in order to allow pharmacokinetics data specific to the individual variants to be integrated into this type of analysis at some point. Because we have no pharmacokinetics data available for A30P, Q31P, and K.O. on ARBC surfaces, H/Ref values were set at 1.0 for all three variants. Thus, the rank-order of the three variants reported herein is entirely based upon differences in SIRP-α-binding retention and antibody escape; the ranking does not reflect differences in predicted circulation half-life. Furthermore, it would be premature to interpret higher affinities for SIRP-α as indicative of prolonged circulation in vivo. Clearance from circulation will be influenced by many other factors including, but not limited to, complement activation, opsonization, macrophage recognition, and physical properties of the particles.

© The National High School Journal of Science 2026

Step 3: Hill equation calibration. Phagocytosis rate P was modeled as a Hill equation in effective surface density ρ_{eff}:

$$P(\rho_{\text{eff}}) = P_{\max} - \Delta P \times \frac{\rho_{\text{eff}}}{\rho_{\text{half}} + \rho_{\text{eff}}} \tag{3}$$

where $P_{\max} = 39.2\%$ and $P_{\min} = 15.5\%$ were derived as grand means of B6H12-blocked and untreated phagocytosis values across all donors and replicates from the published source data[?]. ρ_{half} was estimated by treating CAR-T cells ($\rho_T \approx 60.4$ molecules/μm^2, calculated by dividing the 9,292 molecules per cell reported by Yamada-Hunter et al. by the estimated surface area of a 7 μm-diameter T cell: $4\pi \times 3.5^2 \approx 154$ μm^2) as achieving a target phagocytosis of 20% and solving:

$$\rho_{\text{half}} = \rho_T \times \frac{1-\theta_T}{\theta_T} \approx 14.2 \text{ molecules}/\mu\text{m}^2 \tag{4}$$

The "ρ-half" is an approximate measure for the effective CD47 surface density at which phagocytosis reaches the midpoint between P-max and P-min. It represents the midpoint response between the maximum (P-max) and minimum (P-min) levels of phagocytosis and therefore, does not represent a real-world or measured two-dimensional molecular binding constant but rather an inferred density-scale parameter calibrated from a single assumed CAR-T cell operating point. Due to a lack of sufficient data to fit a dose-response curve to the specific experimental conditions in use for Q31P-CD47 binding to ARBC surfaces, the dose-response curve was not fitted to a full experimental density-response dataset. Therefore, a 25% phagocytosis threshold was selected as a working design target for determining the effect of reduced phagocytosis on ARBC levels due to the fact that there is likely considerable reduction in phagocytosis relative to the fully unprotected state (i.e., P-max = 39.2%) and still somewhat conservative relative to the fully protected state (i.e., P-min = 15.5%). As such, this 25% threshold was selected without validation as being sufficient to allow for adequate ARBC circulation and thus, is considered a modeling assumption. The actual clinically relevant threshold may differ. In addition, the model utilized here was obtained from studies on human CAR-T cells and then transferred to an ARBC system as an approximation; therefore, differences exist between these systems and may include factors such as membrane composition, density of glycocalyx, protein mobility, and their interactions with macrophages, which could impact the accuracy of this approximation[25]. **Step 4: Geometric correction factors.** Total required surface density was related to effective density through:

$$\rho_{\text{eff}} = \rho_{\text{total}} \times f_{\text{orient}} \times f_{\text{steric}} \times f_{\text{curv}} \tag{5}$$

where $f_{\text{orient}} = 0.50$ (random chemical conjugation) or 0.90 (CRISPR transmembrane expression); $f_{\text{steric}} = 0.70$ (estimated steric occlusion by membrane crowding/glycocalyx); and f_{curv} was calculated geometrically for each ARBC diameter as the mean cosine of the angle subtended by the macrophage contact zone (contact area ≈ 1 μm^2 assumed for a rigid sphere).

$f_{\text{curv}} = \cos(\alpha)$, where $\sin(\alpha) = \frac{r_c}{R}$, $r_c = \sqrt{\frac{A_{\text{contact}}}{\pi}}$, R is the ARBC radius, and $A_{\text{contact}} \approx 1$ μm^2.

Data Analysis

All of our calculations were completed in MATLAB R2024a. The complete MATLAB script is provided as Supplementary File S2. We used sensitivity analysis to calculate how different combinations of the diameter of the ARBCs (2–10 μm) and the interaction of both orientation $\times$ steric factors (0.20–1.00) would affect the results. We calculated the results using an 80×80 grid. The dose-response curves were generated for effective surface densities ranging from 0 to 200 molecules per square micron.

Ethical Considerations

The work described in this paper is completely computational and based on previously reported data from experiments. No new human or animal subject experiments were conducted in this study. Institutional Review Board approval was therefore unnecessary for this project. Supplementary Table S1 provides all numerical inputs and their corresponding values and sources, while also identifying whether each value was derived from published data or selected as a modeling assumption.

Results

Circulation decay model

The illustrative first-order exponential decay model using the half-life values reported by Hu et al. as reference anchors ($k_{\text{PEG}} = 0.04387$ h^{-1}; $k_{\text{RBC}} = 0.01750$ h^{-1}) shows that at 24 hours, PEG-coated carriers retain approximately 35% of the initial population, whereas RBC-membrane-coated (CD47-bearing) carriers retain approximately 66% (Figure 1). Therefore, there is a 2.5 fold increase in the half-lives of these two cell types due to the CD47 coating on the RBC membrane and provides the rationale for Q31P-CD47 as an ARBC strategy. It should be noted that the circulation advantage of nanoparticles coated with erythrocyte membranes is due to coating with the entire erythrocyte membrane as opposed to CD47 alone and was shown for nanoparticles $<$100 nm but not micrometer-scale ARBCs.

© The National High School Journal of Science 2026

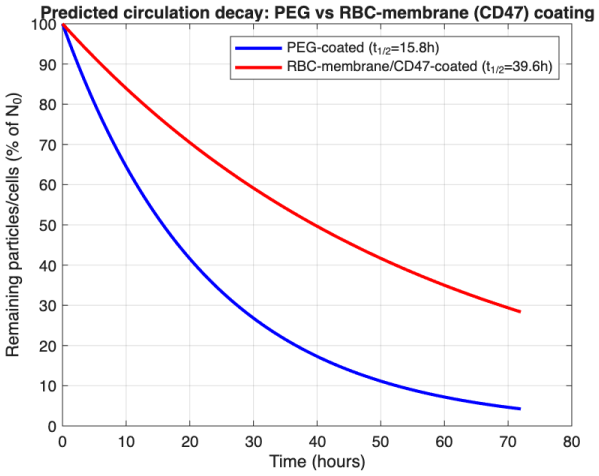


Figure. 1 Predicted exponential circulation decay of PEG-coated ($t_{1/2}$ = 15.8 h) versus RBC-membrane/CD47-coated ($t_{1/2}$ = 39.6 h) nanoparticles over 72 hours, computed from verified clearance constants. Hu et al. provided the half-life values that were used to compute these values using a first-order exponential decay model. This is not a reconstruction of the original two-compartment circulation profile and should be viewed as an illustrative example of how to calculate the values in this table.

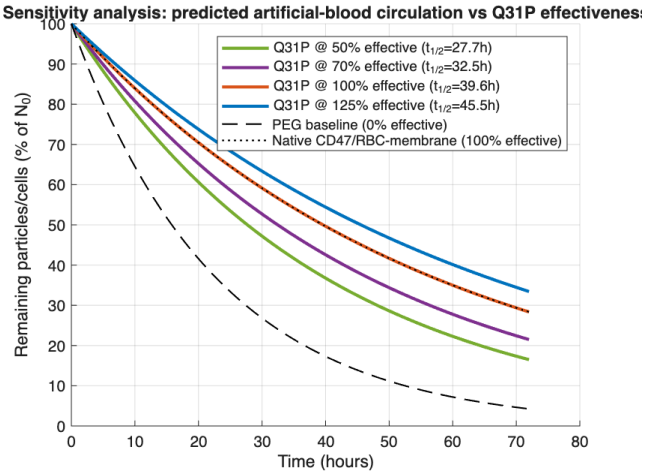


Figure. 2 Sensitivity analysis: predicted circulation decay of Q31P-coated ARBCs across effectiveness scenarios (50-125%), plotted against PEG and RBC-membrane reference curves.

Sensitivity analysis across Q31P effectiveness scenarios

In spite of the low 50% effectiveness assumption, the Q31P-effectiveness scaling model (Table 1, Figure 2), predicts an improved circulation half-life for the Q31P-coated ARBCs of 27.7 hours; which is a 75% increase over those with a coating of PEG. At 100% effectiveness, it was estimated the ARBCs will circulate as long as native CD47 coated carriers (39.6 h). The 125% scenario (a speculative extrapolation as opposed to an anticipated outcome) foresees an increase in circulation half-life to about 45.55 hours.

Table 1 Predicted half-life and clearance constant by Q31P effectiveness scenario.

Q31P effectiveness (%)	Predicted half-life (h)	Clearance constant k (h^{-1})
0 (PEG baseline)	15.80	0.04387
50	27.70	0.02502
70	32.46	0.02135
100 (native CD47)	39.60	0.01750
125	45.55	0.01522

Multi-variant CD47 binding selectivity and SICI comparison

Table 2 and Figure 3 present SICI scores for all three CD47 variants computed from Yamada-Hunter et al.[23] source data. Three findings emerge. First, KO produces SICI ≈ 0, confirming the metric's lower-bound behavior: $S \approx 0$ collapses SICI regardless of antibody values, correctly identifying total loss of immune camouflage.

Second, A30P ranks above Q31P by SICI (1.461 vs. 1.258), a non-obvious result: Q31P is the superior antibody-evader ($A = 0.04\%$ vs. 6.06% for A30P), yet A30P's greater SIRPα engagement more than compensates under the $H = 1.0$ assumption. Third, the two variants represent distinct trade-off profiles: A30P is preferred in standard (no antibody) clinical contexts, while Q31P's near-total antibody resistance ($A = 0.04\%$) makes it uniquely suitable when therapeutic anti-CD47 antibodies are present. In antibody-free contexts, A30P scores higher on the binding-selectivity metric, but there was no evidence to support the conclusion that A30P has a superior circulation half-life relative to Q31P in vivo.

The presence of B6H12 results in Q31P having a substantial binding-selectivity advantage due to the extremely low reactivity of Q31P with B6H12 ($A = 0.04\%$). As these conclusions are specific to the interaction with the antibody B6H12, they may not reflect the binding characteristics of other anti-CD47 antibodies unless additional binding data are available.

Table 2 SICI components and composite scores for three CD47 variants (normalized to WT CD47 = 1.0, $H/H_{\text{ref}} = 1.0$).

Variant	S (hSIRPα, mean)	A (B6H12, mean)	SICI	SICI Range
A30P	1.5549	0.0606	1.461	1.393 – 1.529
Q31P	1.2585	0.000421	1.258	1.156 – 1.360
KO	0.0001	0.000453	≈ 0.000	≈ 0.000

© The National High School Journal of Science 2026

To assess how consistent our results were, SICI was calculated using the average ± one standard deviation (SD) of each set of three replicate K_d measurements. For A30P, we obtained a range of 1.393–1.529; for Q31P, a range of 1.156–1.360. Since these ranges did not intersect with each other, the A30P > Q31P ranking remained stable across the observed measurement variability.

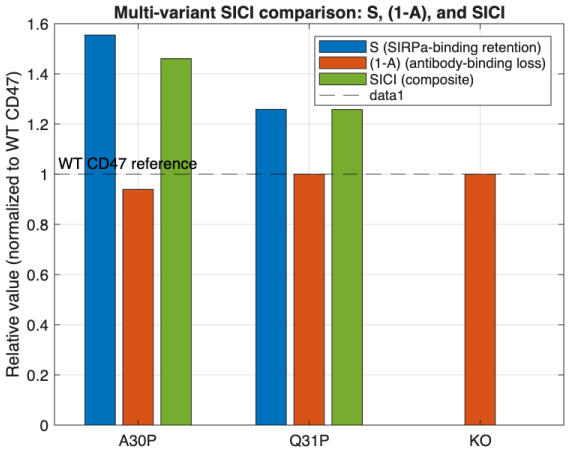


Figure. 3 Multi-variant SICI comparison. Grouped bar chart showing S (SIRPα-binding retention), $(1-A)$ (antibody-binding loss), and SICI composite score for A30P, Q31P, and KO variants, normalized to WT CD47. KO produces SICI ≈ 0 (boundary validation); A30P ranks above Q31P despite Q31P's superior antibody evasion.

Illustrative surface-density design model for ARBC coating

The Hill equation dose-response curve (Figure 4) calibrated by using phagocytosis data collected by Yamada-Hunter et al.[23] yields $\rho_{\text{half}} \approx 14.2$ molecules/μm^2. Also, the effective density threshold at which $P < 25\%$ phagocytosis occurs is $\rho_{\text{eff,threshold}} \approx 21.2$ molecules/μm^2, only 35% of the T-cell operating density (60.4 molecules/μm^2). The estimations in this section are conditional estimates from the developed model that rely upon all of the assumptions stated above. In particular, the coating estimates depend upon (1) calibration from a single assumed operating point, (2) the 25% phagocytosis threshold used as a basis for estimating the amount of Q31P-CD47 required per ARBC, and (3) the assumption that T-cell binding behavior can be transferred to the ARBC surface as an approximation. Therefore, these estimates should not be interpreted as experimentally validated minimum coating requirements. This reveals an important yet non-obvious finding: although CD47 Q31P-expressing T cells have a large number of copies on their surface (9,292 molecules/cell), the number of copies on the surface of these cells defines neither the minimum required quantity of molecules for ARBC's nor the operating point of these T cells within the saturation region of the dose response curve ($\theta \approx 0.81$). As such, ARBCs are not required to be coated with the same degree as T cells. ARBCs do not need to replicate this level of saturation; they only need to reach the threshold.

Table 3

Phagocytosis target	ρ_{eff} (molecules/μm^2)	Random conjugation (N)	CRISPR expression (N)
P < 20%	60.6	~13,720	~7,620
P < 25%	21.1	~4,797	~2,665
P < 30%	9.0	~2,040	~1,130

Although the estimated numbers for a 5 μm ARBC were in the thousands (approximately 1,130 for CRISPR at the 30% target vs. approximately 13,720 for random conjugation at the 20% target), this is also an example of how strongly dependent these estimates are on the selected threshold and, as such, reinforces the conditional nature of these estimates.

For an average (representative) ARBC having a diameter of 5 micrometers (μm) and a total surface area of 78.5 square micrometers (μm^2), random chemical conjugation is estimated to require around 4,797 molecules per ARBC for an orientation factor of 0.50; steric hindrance factors at 0.7; and curvature factors at 0.991. As compared to this number, utilizing CRISPR transmembrane expression with orientation factors at 0.9 reduces the required amount to about 2,665 molecules per ARBC.

Three other design aspects of the two-dimensional sensitivity map shown in Figure 5 are evident. First, because $f_{\text{curv}} \geq 0.991$ for all ARBC diameters 3–9 μm, curvature of the membrane can be considered to be negligible. Second, required molecule count scales quadratically with ARBC diameter: a 9 μm ARBC requires 3.2-fold more CD47 than a 5 μm ARBC. Third, the combined orientation × steric factor shows diminishing returns above 0.6: improving from 0.2 to 0.6 reduces required molecules by 67%, while improving from 0.6 to 1.0 reduces it by only 40%.

Conclusion

Restatement of Key Findings

The research provided several key results. The first was that pharmacokinetics indicated that based on coating efficiency, Q31P-CD47 coated ARBCs would have circulating half-lives of 27.7–45.6 hours, which represented a 75%–189% increase in half-life when compared to PEGylated ARBCs.

The second result was that SICI analysis of three CD47 variants demonstrated a non-obvious ranking: overall A30P

© The National High School Journal of Science 2026

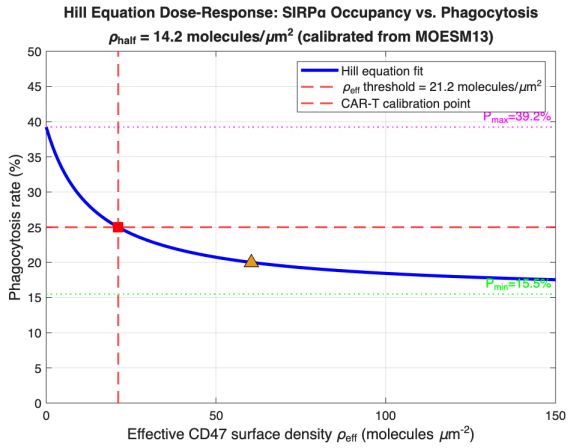


Figure. 4 Hill equation dose-response: phagocytosis rate $P(\%)$ versus effective CD47 surface density ρ_{eff} (molecules/μm^2). Red dashed lines mark the ρ_{eff} threshold for $P < 25\%$. Orange triangle: CAR-T cell calibration point ($\rho = 60.4$ molecules/μm^2, $P \approx 20\%$). Green/magenta dotted lines: P_{min} and P_{max} from published data.

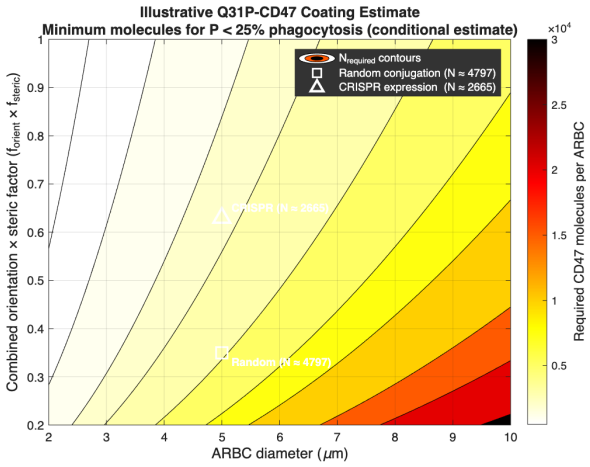


Figure. 5 Two-dimensional design map of required Q31P-CD47 molecules per ARBC as a function of ARBC diameter (μm) and combined orientation $\times$ steric factor. White markers indicate operating points for a 5 μm ARBC under random conjugation (square, $N \approx 4{,}797$) and CRISPR expression (triangle, $N \approx 2{,}665$).

scored as highest with a score of 1.461; however, within the context of using antibodies against CD47 for therapeutic purposes, Q31P (score = 1.258) is the most favorable variant - a difference unapparent from individual parameters alone. Finally, the Hill equation surface density model predicted that Q31P-CD47 coated ARBCs required only 2,665–4,797 Q31P-CD47 molecules per cell when comparing CRISPR and random conjugation approaches, respectively.

These values are dramatically lower than the 9,292 molecules/cells reported to protect CAR-T cells.

Implications and Significance

The main contribution of this research is in combining previous evidence on circulating benefits of CD47 bearing biomimetic coatings [12,16,17] and the multi-variant receptor selectivity results for engineered CD47 to produce an integrated quantitative framework. Alone neither dataset can support claims regarding artificial blood, but together, they allow for specific predictions as well as a screening tool (SICI) to evaluate these predictions.

The T-cell saturation result directly impacts engineering due to T cells being in an 81% occupied state with respect to receptors, despite the model predicting that only ∼60% receptor occupancy is required to achieve a phagocytosis rate $P < 25\%$; therefore, there are "excess" CD47s on T cells from an ARBC engineering perspective. The Hill equation represents the true threshold (and not the operating conditions of the T-cell), while also indicating that orientation control (versus curvature adjustment) is the primary mechanism through which the potential recovery of excess CD47 via rational conjugate design will occur.

The SICI framework's context-dependent ranking directly addresses an unresolved clinical design question. In situations with no antibodies, including trauma or perioperative contexts, A30P has a higher score on the SICI binding-selectivity metric. This does not prove that A30P will circulate longer in vivo because there are many factors in addition to SIRPα engagement that affect how long it remains in circulation. In oncology scenarios where patients receive therapeutic anti-CD47 antibodies, Q31P's near-zero antibody reactivity ($A = 0.04\%$) prevents antibody-mediated stripping of the 'don't eat me' signal, making Q31P a coating option with a binding-selectivity advantage as a result of its lower reactivity with B6H12 in contexts where B6H12 is present, based on the available binding data. This distinction cannot be derived from either S or A individually, it emerges from the multiplicative structure of SICI.

Connection to Objectives

The three research questions were each addressed. (1) Half-lives for predicted Q31P ranges from 27.7 h (50% effectiveness) to 45.6 hours (125%). The 100% scenario represents an upper-bound assumption for a Q31P-CD47 coating by assuming it has the same circulation benefits as if it were coated with the entire membrane from an RBC. On the other hand, the 125% scenario extends beyond the 100% scenario by being a speculative extension; it should not be taken as an expected biological outcome. The influence of SIRPα interaction strength does not necessarily directly correlate with a

© The National High School Journal of Science 2026

proportional increase in circulation half-life due to the multitude of clearance mechanisms beyond just SIRPα interaction, such as activation of the complement system, opsonization, and physical properties of particles[26]. (2) A non-trivial ordering (A30P $>$ Q31P $>$ KO) was found using SICI which will depend upon the patient's medical history. (3) Based upon the molecular orientation of the membrane, there are approximately 2,665–4,797 molecules required to coat an ARBC; and membrane curvature has been determined to be a very minor influence ($<$1%).

Recommendations

Several directly testable predictions follow from this framework. First, both A30P- and Q31P-coated ARBCs should be produced and their circulation half-lives measured in vivo, allowing direct comparison against Figure 2 curves. If the SICI ranking (A30P $>$ Q31P without antibody; Q31P preferred under antibody challenge) holds experimentally, it would provide the first empirical validation of SICI as a predictive metric. Second, phagocytosis assays using ARBCs coated at 1,000–8,000 CD47 molecules/cell would directly test the Hill equation dose-response calibration; a phagocytosis rate below 25% at approximately 2,700–4,800 molecules/cell would confirm the model's prediction. Third, SIRPα and B6H12 binding should be re-measured in the ARBC membrane context to refine S and A beyond the T-cell-derived values used here.

Limitations

There are five major constraints to how strong the conclusions of this research are; first, there are no available data on direct circulation for Q31P-coated ARBCs. Therefore, the predicted half-lives in this work are model projections based on linear interpolation instead of actual experimental measurements. Second, transferring binding data from one biological environment to another has some degree of uncertainty since the SIRPα and B6H12 binding measurements were obtained using human T cells rather than yeast-derived ARBC surfaces; differences in such things as membrane composition, glycosylation, and surface density may alter the effective S and A values on ARBCs. Third, the assumption that coating effectiveness scales linearly is an oversimplification because circulation half-life can be influenced by a complex combination of factors, including opsonization, complement activation, and mechanical filtration. The use of linear interpolation may not capture nonlinearities or threshold effects that can occur in vivo. Fourth, $f_{\text{steric}} = 0.70$ is an estimate based upon general considerations of membrane crowding rather than a value actually measured on yeast-derived ARBC surfaces. Fifth, the previously reported circulation half-life of about 30 hours for uncoated ARBCs was excluded because the cited source could not be verified, leaving a gap in the comparison baseline.

Closing Thought

A major obstacle in artificial blood development has been translating many successful examples of molecular biology into quantifiable engineering specifications that can guide future experiments. This study demonstrates how combining existing pharmacokinetic data with receptor occupancy theory can facilitate translation of these expectations into actionable engineering targets: a specific variant, a specific molecule count, and a context-specific rationale. The predictions made here are directly testable, and the SICI framework is extensible to future CD47 variants as binding data become available, turning a one-time calculation into a reusable rational design tool for immune-camouflage engineering.

References

1 T. M. S. Chang, From artificial red blood cells, oxygen carriers, and oxygen therapeutics to artificial cells, nanomedicine, and beyond. Artificial Cells, Blood Substitutes and Immobilization Biotechnology. Vol. 40, pg. 197–199, 2012., https://doi.org/10.3109/10731199.2012.662408.

2 M. Cao, et al., New applications of HBOC-201: a 25-year review of the literature. Frontiers in Medicine. Vol. 8, art. 794561, 2021., https://doi.org/10.3389/fmed.2021.794561.

3 R. M. Winslow, Current status of oxygen carriers ('blood substitutes'): 2006. Vox Sanguinis. Vol. 91, pg. 102–110, 2006., https://doi.org/10.1111/j.1423-0410.2006.00789.x.

4 A. T. Frost, I. H. Jacobsen, A. Worberg, J. L. Martínez, How synthetic biology and metabolic engineering can boost the generation of artificial blood using microbial production hosts. Frontiers in Bioengineering and Biotechnology. Vol. 6, pg. 186, 2018., https://doi.org/10.3389/fbioe.2018.00186.

5 H. Bloomer, J. Khirallah, Y. Li, Q. Xu, CRISPR/Cas9 ribonucleoprotein-mediated genome and epigenome editing in mammalian cells. Advanced Drug Delivery Reviews. Vol. 181, pg. 114087, 2022., https://doi.org/10.1016/j.addr.2021.114087.

6 F. Alexis, et al., Factors affecting the clearance and biodistribution of polymeric nanoparticles. Molecular Pharmaceutics. Vol. 5, pg. 505–515, 2008., https://doi.org/10.1021/mp800051m.

7 P. A. Oldenborg, A. Zheleznyak, Y. F. Fang, C. F. Lagenaur, H. D. Gresham, F. P. Lindberg, Role of CD47 as a marker of self on red blood cells. Science. Vol. 288, pg. 2051–2054, 2000., https://doi.org/10.1126/science.288.5473.2051.

8 E. J. Brown, W. A. Frazier, Integrin-associated protein (CD47) and its ligands. Trends in Cell Biology. Vol. 11, pg. 130–135, 2001., https://doi.org/10.1016/S0962-8924(00)01906-1.

9 T. Matozaki, et al., Functions and molecular mechanisms of the CD47–SIRPα signalling pathway. Trends in Cell Biology. Vol. 19, pg. 72–80, 2009., https://doi.org/10.1016/j.tcb.2008.12.001.

10 R. K. Tsai, D. E. Discher, Inhibition of "self" engulfment through deactivation of myosin-II at the phagocytic synapse between human cells. Journal of Cell Biology. Vol. 180, pg. 989–1003, 2008., https://doi.org/10.1083/jcb.200708043.

11 A. N. Barclay, T. K. Van den Berg, The interaction between signal regulatory protein alpha (SIRPα) and CD47: structure, function, and therapeutic target. Annual Review of Immunology. Vol. 32, pg. 25–50, 2014.,

© The National High School Journal of Science 2026

https://doi.org/10.1146/annurev-immunol-032713-120142.

12 C. M. J. Hu, L. Zhang, S. Aryal, C. Cheung, R. H. Fang, L. Zhang, Erythrocyte membrane-camouflaged polymeric nanoparticles for biomimetic delivery vehicles. Proceedings of the National Academy of Sciences. Vol. 108, pg. 10980–10985, 2011., https://doi.org/10.1073/pnas.1106634108.

13 J. J. F. Verhoef, T. J. Anchordoquy, Questioning the use of PEGylation for drug delivery. Drug Delivery and Translational Research. Vol. 3, pg. 499–503, 2013., https://doi.org/10.1007/s13346-013-0176-5.

14 B. T. Luk, L. Zhang, Cell membrane-camouflaged nanoparticles for drug delivery. Journal of Controlled Release. Vol. 220, pg. 600–607, 2015., https://doi.org/10.1016/j.jconrel.2015.07.019.

15 P. L. Rodriguez, et al., Minimal "self" peptides that inhibit phagocytic clearance and enhance delivery of nanoparticles. Science. Vol. 339, pg. 971–975, 2013., https://doi.org/10.1126/science.1229568.

16 C.-M. J. Hu, et al., 'Marker-of-self' functionalization of nanoscale particles through a top-down cellular membrane coating approach. Nanoscale. Vol. 5, pg. 2664–2668, 2013., https://doi.org/10.1039/c3nr00015j.

17 Y. Qie, et al., Surface modification of nanoparticles enables selective evasion of phagocytic clearance by distinct macrophage phenotypes. Scientific Reports. Vol. 6, art. 26269, 2016., https://doi.org/10.1038/srep26269.

18 S. B. Willingham, et al., The CD47-signal regulatory protein alpha (SIRPα) interaction is a therapeutic target for human solid tumors. Proceedings of the National Academy of Sciences. Vol. 109, pg. 6662–6667, 2012., https://doi.org/10.1073/pnas.1121623109.

19 M. P. Chao, I. L. Weissman, R. Majeti, The CD47–SIRPα pathway in cancer immune evasion and potential therapeutic implications. Current Opinion in Immunology. Vol. 24, pg. 225–232, 2012., https://doi.org/10.1016/j.coi.2012.01.010.

20 R. Advani, et al., CD47 blockade by Hu5F9-G4 and rituximab in non-Hodgkin's lymphoma. New England Journal of Medicine. Vol. 379, pg. 1711–1721, 2018., https://doi.org/10.1056/NEJMoa1807315.

21 W. Zhang, et al., Advances in anti-tumor treatments targeting the CD47/SIRPα axis. Frontiers in Immunology. Vol. 11, art. 18, 2020., https://doi.org/10.3389/fimmu.2020.00018.

22 R. Maute, et al., CD47–SIRPα-targeted therapeutics: status and prospects. Immuno-Oncology and Technology. Vol. 13, 2022., https://pmc.ncbi.nlm.nih.gov/articles/PMC9216458/.

23 S. A. Yamada-Hunter, et al., Engineered CD47 protects T cells for enhanced antitumour immunity. Nature. Vol. 630, pg. 457–465, 2024., https://doi.org/10.1038/s41586-024-07443-8.

24 R. K. Tsai, D. E. Discher, Self inhibition of phagocytosis: the affinity of 'marker of self' CD47 for SIRPα dictates potency of inhibition but only at low expression levels. Blood Cells, Molecules, and Diseases. Vol. 45, pg. 67–74, 2010., https://doi.org/10.1016/j.bcmd.2010.02.016.

25 N. G. Sosale, et al., Cell rigidity and shape override CD47's "self"-signaling in phagocytosis by hyperactivating myosin-II. Blood. Vol. 125, pg. 542–552, 2015., https://doi.org/10.1182/blood-2014-06-585299.

26 P.-A. Oldenborg, et al., CD47–signal regulatory protein alpha (SIRPα) regulates Fcγ and complement receptor-mediated phagocytosis. Journal of Experimental Medicine. Vol. 193, pg. 855–861, 2001., https://doi.org/10.1084/jem.193.7.855.

© The National High School Journal of Science 2026

Supplementary Information

Table S1 Numerical inputs used in the computational model.

Parameter	Symbol	Value	Source	Measured or assumed
PEG half-life	$t_{1/2,\mathrm{PEG}}$	15.8 h	Hu et al.	Measured
RBC membrane half-life	$t_{1/2,\mathrm{RBC}}$	39.6 h	Hu et al.	Measured
PEG clearance constant	k_{PEG}	0.04387 h^{-1}	Derived from $t_{1/2,\mathrm{PEG}}$	Derived
RBC clearance constant	k_{RBC}	0.01750 h^{-1}	Derived from $t_{1/2,\mathrm{RBC}}$	Derived
Q31P effectiveness scenarios	–	50%, 70%, 100%, 125%	–	Assumed
hSIRPα binding, A30P	S	1.5549	Yamada-Hunter et al.	Measured
hSIRPα binding, Q31P	S	1.2585	Yamada-Hunter et al.	Measured
hSIRPα binding, KO	S	0.0001	Yamada-Hunter et al.	Measured
B6H12 binding, A30P	A	0.0606	Yamada-Hunter et al.	Measured
B6H12 binding, Q31P	A	0.000421	Yamada-Hunter et al.	Measured
B6H12 binding, KO	A	0.000453	Yamada-Hunter et al.	Measured
H/Href (all variants)	H/Href	1.0	—	Assumed
Maximum phagocytosis	$P_{\max}$	39.2%	Yamada-Hunter et al.	Derived (grand mean)
Minimum phagocytosis	$P_{\min}$	15.5%	Yamada-Hunter et al.	Derived (grand mean)
CD47 molecules per CAR-T cell	–	9,292	Yamada-Hunter et al.	Measured
T cell diameter	–	7 μm	–	Assumed
T cell surface area	–	154 $\mu\mathrm{m}^2$	–	Derived
CAR-T surface density	ρ_T	60.4 molecules/$\mu\mathrm{m}^2$	Derived from Yamada-Hunter et al.	Derived
Calibration phagocytosis target	–	20%	–	Assumed
Half-response surface density	ρ_{half}	14.2 molecules/$\mu\mathrm{m}^2$	–	Derived
Phagocytosis suppression threshold	–	25%	–	Assumed
Orientation factor, random conjugation	f_{orient}	0.50	–	Assumed
Orientation factor, CRISPR expression	f_{orient}	0.90	–	Assumed
Steric correction factor	f_{steric}	0.70	–	Assumed
Macrophage contact area	A_{contact}	1 $\mu\mathrm{m}^2$	–	Assumed
Representative ARBC diameter	–	5 μm	–	Assumed
ARBC surface area (5 μm)	–	78.5 $\mu\mathrm{m}^2$	–	Derived
ARBC diameter range (sensitivity)	–	2–10 μm	–	Assumed

© The National High School Journal of Science 2026